

Measurement of branching fractions of  $D_s^+ \rightarrow K_S^0 K_S^0 \pi^+ \pi^0$  and  $D_s^+ \rightarrow K_S^0 K^+ \pi^0 \pi^0$ 

M. Ablikim<sup>1</sup>, M. N. Achasov<sup>4,b</sup>, P. Adlarson<sup>79</sup>, X. C. Ai<sup>84</sup>, R. Aliberti<sup>37</sup>, A. Amoroso<sup>78A,78C</sup>, Q. An<sup>75,61,t</sup>, Y. Bai<sup>60</sup>, O. Bakina<sup>38</sup>, Y. Ban<sup>48,g</sup>, H.-R. Bao<sup>67</sup>, V. Batozskaya<sup>1,46</sup>, K. Begzsuren<sup>34</sup>, N. Berger<sup>37</sup>, M. Berlowski<sup>46</sup>, M. B. Bertani<sup>30A</sup>, D. Bettoni<sup>31A</sup>, F. Bianchi<sup>78A,78C</sup>, E. Bianco<sup>78A,78C</sup>, A. Bortone<sup>78A,78C</sup>, I. Boyko<sup>38</sup>, R. A. Briere<sup>5</sup>, A. Brueggemann<sup>72</sup>, H. Cai<sup>80</sup>, M. H. Cai<sup>40,j,k</sup>, X. Cai<sup>1,61</sup>, A. Calcaterra<sup>30A</sup>, G. F. Cao<sup>1,67</sup>, N. Cao<sup>1,67</sup>, S. A. Cetin<sup>65A</sup>, X. Y. Chai<sup>48,g</sup>, J. F. Chang<sup>1,61</sup>, T. T. Chang<sup>45</sup>, G. R. Che<sup>45</sup>, Y. Z. Che<sup>1,61,67</sup>, C. H. Chen<sup>9</sup>, Chao Chen<sup>58</sup>, G. Chen<sup>1</sup>, H. S. Chen<sup>1,67</sup>, H. Y. Chen<sup>21</sup>, M. L. Chen<sup>1,61,67</sup>, S. J. Chen<sup>44</sup>, S. M. Chen<sup>64</sup>, T. Chen<sup>1,67</sup>, X. R. Chen<sup>33,67</sup>, X. T. Chen<sup>1,67</sup>, X. Y. Chen<sup>12,f</sup>, Y. B. Chen<sup>1,61</sup>, Y. Q. Chen<sup>16</sup>, Z. K. Chen<sup>62</sup>, J. C. Cheng<sup>47</sup>, L. N. Cheng<sup>45</sup>, S. K. Choi<sup>10</sup>, X. Chu<sup>12,f</sup>, G. C. Cibinetto<sup>31A</sup>, F. Cossio<sup>78C</sup>, J. Cottee-Meldrum<sup>66</sup>, H. L. Dai<sup>1,61</sup>, J. P. Dai<sup>82</sup>, X. C. Dai<sup>64</sup>, A. Dbeysy<sup>19</sup>, R. E. de Boer<sup>3</sup>, D. Dedovich<sup>38</sup>, C. Q. Deng<sup>76</sup>, Z. Y. Deng<sup>1</sup>, A. Denig<sup>37</sup>, I. Denisenko<sup>38</sup>, M. Destefanis<sup>78A,78C</sup>, F. De Mori<sup>78A,78C</sup>, X. X. Ding<sup>48,g</sup>, Y. Ding<sup>42</sup>, Y. X. Ding<sup>32</sup>, J. Dong<sup>1,61</sup>, L. Y. Dong<sup>1,67</sup>, M. Y. Dong<sup>1,61,67</sup>, X. Dong<sup>80</sup>, M. C. Du<sup>1</sup>, S. X. Du<sup>84</sup>, S. X. Du<sup>12,f</sup>, X. L. Du<sup>84</sup>, Y. Y. Duan<sup>58</sup>, Z. H. Duan<sup>44</sup>, P. Egorov<sup>38,a</sup>, G. F. Fan<sup>44</sup>, J. J. Fan<sup>20</sup>, Y. H. Fan<sup>47</sup>, J. Fang<sup>1,61</sup>, J. Fang<sup>62</sup>, S. S. Fang<sup>1,67</sup>, W. X. Fang<sup>1</sup>, Y. Q. Fang<sup>1,61</sup>, L. Fava<sup>78B,78C</sup>, F. Feldbauer<sup>3</sup>, G. Felici<sup>30A</sup>, C. Q. Feng<sup>75,61</sup>, J. H. Feng<sup>16</sup>, L. Feng<sup>40,j,k</sup>, Q. X. Feng<sup>40,j,k</sup>, Y. T. Feng<sup>75,61</sup>, M. Fritsch<sup>3</sup>, C. D. Fu<sup>1</sup>, J. L. Fu<sup>67</sup>, Y. W. Fu<sup>1,67</sup>, H. Gao<sup>67</sup>, Y. Gao<sup>75,61</sup>, Y. N. Gao<sup>48,g</sup>, Y. N. Gao<sup>20</sup>, Y. Y. Gao<sup>32</sup>, Z. Gao<sup>45</sup>, S. Garbolino<sup>78C</sup>, I. Garzia<sup>31A,31B</sup>, L. Ge<sup>60</sup>, P. T. Ge<sup>20</sup>, Z. W. Ge<sup>44</sup>, C. Geng<sup>62</sup>, E. M. Gersabeck<sup>71</sup>, A. Gilman<sup>73</sup>, K. Goetzen<sup>13</sup>, J. D. Gong<sup>36</sup>, L. Gong<sup>42</sup>, W. X. Gong<sup>1,61</sup>, W. Gradl<sup>37</sup>, S. Gramigna<sup>31A,31B</sup>, M. Greco<sup>78A,78C</sup>, M. D. Gu<sup>53</sup>, M. H. Gu<sup>1,61</sup>, C. Y. Guan<sup>1,67</sup>, A. Q. Guo<sup>33</sup>, J. N. Guo<sup>12,f</sup>, L. B. Guo<sup>43</sup>, M. J. Guo<sup>52</sup>, R. P. Guo<sup>51</sup>, X. Guo<sup>52</sup>, Y. P. Guo<sup>12,f</sup>, A. Guskov<sup>38,a</sup>, J. Gutierrez<sup>29</sup>, T. T. Han<sup>1</sup>, F. Hanisch<sup>3</sup>, K. D. Hao<sup>75,61</sup>, X. Q. Hao<sup>20</sup>, F. A. Harris<sup>69</sup>, C. Z. He<sup>48,g</sup>, K. L. He<sup>1,67</sup>, F. H. Heinsius<sup>3</sup>, C. H. Heinz<sup>37</sup>, Y. K. Heng<sup>1,61,67</sup>, C. Herold<sup>63</sup>, P. C. Hong<sup>36</sup>, G. Y. Hou<sup>1,67</sup>, X. T. Hou<sup>1,67</sup>, Y. R. Hou<sup>67</sup>, Z. L. Hou<sup>1</sup>, H. M. Hu<sup>1,67</sup>, J. F. Hu<sup>59,i</sup>, Q. P. Hu<sup>75,61</sup>, S. L. Hu<sup>12,f</sup>, T. Hu<sup>1,61,67</sup>, Y. Hu<sup>1</sup>, Z. M. Hu<sup>62</sup>, G. S. Huang<sup>75,61</sup>, K. X. Huang<sup>62</sup>, L. Q. Huang<sup>33,67</sup>, P. Huang<sup>44</sup>, X. T. Huang<sup>52</sup>, Y. P. Huang<sup>1</sup>, Y. S. Huang<sup>62</sup>, T. Hussain<sup>77</sup>, N. Hüskens<sup>37</sup>, N. in der Wiesche<sup>72</sup>, J. Jackson<sup>29</sup>, Q. Ji<sup>1</sup>, Q. P. Ji<sup>20</sup>, W. Ji<sup>1,67</sup>, X. B. Ji<sup>1,67</sup>, X. L. Ji<sup>1,61</sup>, X. Q. Jia<sup>52</sup>, Z. K. Jia<sup>75,61</sup>, D. Jiang<sup>1,67</sup>, H. B. Jiang<sup>80</sup>, P. C. Jiang<sup>48,g</sup>, S. J. Jiang<sup>9</sup>, X. S. Jiang<sup>1,61,67</sup>, Y. Jiang<sup>67</sup>, J. B. Jiao<sup>52</sup>, J. K. Jiao<sup>36</sup>, Z. Jiao<sup>25</sup>, S. Jin<sup>44</sup>, Y. Jin<sup>70</sup>, M. Q. Jing<sup>1,67</sup>, X. M. Jing<sup>67</sup>, T. Johansson<sup>79</sup>, S. Kabana<sup>35</sup>, N. Kalantar-Nayestanaki<sup>68</sup>, X. L. Kang<sup>9</sup>, X. S. Kang<sup>42</sup>, M. Kavatsyuk<sup>68</sup>, B. C. Ke<sup>84</sup>, V. Khachatryan<sup>29</sup>, A. Khoukaz<sup>72</sup>, O. B. Kolcu<sup>65A</sup>, B. Kopf<sup>3</sup>, M. Kuessner<sup>3</sup>, X. Kui<sup>1,67</sup>, N. Kumar<sup>28</sup>, A. Kupsc<sup>46,79</sup>, W. Kühn<sup>39</sup>, Q. Lan<sup>76</sup>, W. N. Lan<sup>20</sup>, T. T. Lei<sup>75,61</sup>, M. Lellmann<sup>37</sup>, T. Lenz<sup>37</sup>, C. Li<sup>49</sup>, C. Li<sup>45</sup>, C. H. Li<sup>43</sup>, C. K. Li<sup>21</sup>, D. M. Li<sup>84</sup>, F. Li<sup>1,61</sup>, G. Li<sup>1</sup>, H. B. Li<sup>1,67</sup>, H. J. Li<sup>20</sup>, H. L. Li<sup>84</sup>, H. N. Li<sup>59,i</sup>, Hui Li<sup>45</sup>, J. R. Li<sup>64</sup>, J. S. Li<sup>62</sup>, J. W. Li<sup>52</sup>, K. Li<sup>1</sup>, K. L. Li<sup>40,j,k</sup>, L. J. Li<sup>1,67</sup>, Lei Li<sup>50</sup>, M. H. Li<sup>45</sup>, M. R. Li<sup>1,67</sup>, P. L. Li<sup>67</sup>, P. R. Li<sup>40,j,k</sup>, Q. M. Li<sup>1,67</sup>, Q. X. Li<sup>52</sup>, R. Li<sup>18,33</sup>, S. X. Li<sup>12</sup>, Shanshan Li<sup>27,h</sup>, T. Li<sup>52</sup>, T. Y. Li<sup>45</sup>, W. D. Li<sup>1,67</sup>, W. G. Li<sup>1,t</sup>, X. Li<sup>1,67</sup>, X. H. Li<sup>75,61</sup>, X. K. Li<sup>48,g</sup>, X. L. Li<sup>52</sup>, X. Y. Li<sup>1,8</sup>, X. Z. Li<sup>62</sup>, Y. Li<sup>20</sup>, Y. G. Li<sup>48,g</sup>, Y. P. Li<sup>36</sup>, Z. H. Li<sup>40</sup>, Z. J. Li<sup>62</sup>, Z. X. Li<sup>45</sup>, Z. Y. Li<sup>82</sup>, C. Liang<sup>44</sup>, H. Liang<sup>75,61</sup>, Y. F. Liang<sup>57</sup>, Y. T. Liang<sup>33,67</sup>, G. R. Liao<sup>14</sup>, L. B. Liao<sup>62</sup>, M. H. Liao<sup>62</sup>, Y. P. Liao<sup>1,67</sup>, J. Libby<sup>28</sup>, A. Limphirat<sup>63</sup>, D. X. Lin<sup>33,67</sup>, L. Q. Lin<sup>41</sup>, T. Lin<sup>1</sup>, B. J. Liu<sup>1</sup>, B. X. Liu<sup>80</sup>, C. X. Liu<sup>1</sup>, F. Liu<sup>1</sup>, F. H. Liu<sup>56</sup>, Feng Liu<sup>6</sup>, G. M. Liu<sup>59,i</sup>, H. Liu<sup>40,j,k</sup>, H. B. Liu<sup>15</sup>, H. H. Liu<sup>1</sup>, H. M. Liu<sup>1,67</sup>, Huihui Liu<sup>22</sup>, J. B. Liu<sup>75,61</sup>, J. J. Liu<sup>21</sup>, K. Liu<sup>40,j,k</sup>, K. Liu<sup>76</sup>, K. Y. Liu<sup>42</sup>, Ke Liu<sup>23</sup>, L. Liu<sup>40</sup>, L. C. Liu<sup>45</sup>, Lu Liu<sup>45</sup>, M. H. Liu<sup>36</sup>, P. L. Liu<sup>1</sup>, Q. Liu<sup>67</sup>, S. B. Liu<sup>75,61</sup>, W. M. Liu<sup>75,61</sup>, W. T. Liu<sup>41</sup>, X. L. Liu<sup>40,j,k</sup>, X. K. Liu<sup>40,j,k</sup>, X. L. Liu<sup>12,f</sup>, X. Y. Liu<sup>80</sup>, Y. Liu<sup>40,j,k</sup>, Y. Liu<sup>84</sup>, Y. B. Liu<sup>45</sup>, Z. A. Liu<sup>1,61,67</sup>, Z. D. Liu<sup>9</sup>, Z. Q. Liu<sup>52</sup>, Z. Y. Liu<sup>40</sup>, X. C. Lou<sup>1,61,67</sup>, H. J. Lu<sup>25</sup>, J. G. Lu<sup>1,61</sup>, X. L. Lu<sup>16</sup>, Y. Lu<sup>7</sup>, Y. H. Lu<sup>1,67</sup>, Y. P. Lu<sup>1,61</sup>, Z. H. Lu<sup>1,67</sup>, C. L. Luo<sup>43</sup>, J. R. Luo<sup>62</sup>, J. S. Luo<sup>1,67</sup>, M. X. Luo<sup>83</sup>, T. Luo<sup>12,f</sup>, X. L. Luo<sup>1,61</sup>, Z. Y. Lv<sup>23</sup>, X. R. Lyu<sup>67,o</sup>, Y. F. Lyu<sup>45</sup>, Y. H. Lyu<sup>84</sup>, F. C. Ma<sup>42</sup>, H. L. Ma<sup>1</sup>, Heng Ma<sup>27,h</sup>, J. L. Ma<sup>1,67</sup>, L. L. Ma<sup>52</sup>, L. R. Ma<sup>70</sup>, Q. M. Ma<sup>1</sup>, R. Q. Ma<sup>1,67</sup>, R. Y. Ma<sup>20</sup>, T. Ma<sup>75,61</sup>, X. T. Ma<sup>1,67</sup>, X. Y. Ma<sup>1,61</sup>, Y. M. Ma<sup>33</sup>, F. E. Maas<sup>19</sup>, I. MacKay<sup>73</sup>, M. Maggiora<sup>78A,78C</sup>, S. Malde<sup>73</sup>, Q. A. Malik<sup>77</sup>, H. X. Mao<sup>40,j,k</sup>, Y. J. Mao<sup>48,g</sup>, Z. P. Mao<sup>1</sup>, S. Marcello<sup>78A,78C</sup>, A. Marshall<sup>66</sup>, F. M. Melendi<sup>31A,31B</sup>, Y. H. Meng<sup>67</sup>, Z. X. Meng<sup>70</sup>, G. Mezzadri<sup>31A</sup>, H. Miao<sup>1,67</sup>, T. J. Min<sup>44</sup>, R. E. Mitchell<sup>29</sup>, X. H. Mo<sup>1,61,67</sup>, B. Moses<sup>29</sup>, N. Yu. Muchnoi<sup>4,b</sup>, J. Muskalla<sup>37</sup>, Y. Nefedov<sup>38</sup>, F. Nerling<sup>19,d</sup>, Z. Ning<sup>1,61</sup>, S. Nisar<sup>11,l</sup>, Q. L. Niu<sup>40,j,k</sup>, W. D. Niu<sup>12,f</sup>, Y. Niu<sup>52</sup>, C. Normand<sup>66</sup>, S. L. Olsen<sup>10,67</sup>, Q. Ouyang<sup>1,61,67</sup>, S. Pacetti<sup>30B,30C</sup>, X. Pan<sup>58</sup>, Y. Pan<sup>60</sup>, A. Pathak<sup>10</sup>, Y. P. Pei<sup>75,61</sup>, M. Pelizaeus<sup>3</sup>, H. P. Peng<sup>75,61</sup>, X. J. Peng<sup>40,j,k</sup>, Y. Y. Peng<sup>40,j,k</sup>, K. Peters<sup>13,d</sup>, K. Petridis<sup>66</sup>, J. L. Ping<sup>43</sup>, R. G. Ping<sup>1,67</sup>, S. Plura<sup>37</sup>, V. Prasad<sup>36</sup>, F. Z. Qi<sup>1</sup>, H. R. Qi<sup>64</sup>, M. Qi<sup>44</sup>, S. Qian<sup>1,61</sup>, W. B. Qian<sup>67</sup>, C. F. Qiao<sup>67</sup>, J. H. Qiao<sup>20</sup>, J. J. Qin<sup>76</sup>, J. L. Qin<sup>58</sup>, L. Q. Qin<sup>14</sup>, L. Y. Qin<sup>75,61</sup>, P. B. Qin<sup>76</sup>, X. P. Qin<sup>41</sup>, X. S. Qin<sup>52</sup>, Z. H. Qin<sup>1,61</sup>, J. F. Qiu<sup>1</sup>, Z. H. Qu<sup>76</sup>, J. Rademacker<sup>66</sup>, C. F. Redmer<sup>37</sup>, A. Rivetti<sup>78C</sup>, M. Rolo<sup>78C</sup>, G. Rong<sup>1,67</sup>, S. S. Rong<sup>1,67</sup>, F. Rosini<sup>30B,30C</sup>, Ch. Rosner<sup>19</sup>, M. Q. Ruan<sup>1,61</sup>, N. Salone<sup>46,p</sup>, A. Sarantsev<sup>38,c</sup>, Y. Schelhaas<sup>37</sup>, K. Schoenning<sup>79</sup>, M. Scodiggio<sup>31A</sup>, W. Shan<sup>26</sup>, X. Y. Shan<sup>75,61</sup>, Z. J. Shang<sup>40,j,k</sup>, J. F. Shanguan<sup>17</sup>, L. G. Shao<sup>1,67</sup>, M. Shao<sup>75,61</sup>, C. P. Shen<sup>12,f</sup>, H. F. Shen<sup>1,8</sup>, W. H. Shen<sup>67</sup>, X. Y. Shen<sup>1,67</sup>, B. A. Shi<sup>67</sup>, H. Shi<sup>75,61</sup>, J. L. Shi<sup>12,f</sup>, J. Y. Shi<sup>1</sup>, S. Y. Shi<sup>76</sup>, X. Shi<sup>1,61</sup>, H. L. Song<sup>75,61</sup>, J. J. Song<sup>20</sup>, M. H. Song<sup>40</sup>, T. Z. Song<sup>62</sup>, W. M. Song<sup>36</sup>, Y. X. Song<sup>48,g,m</sup>, Zirong Song<sup>27,h</sup>, S. Sosio<sup>78A,78C</sup>, S. Spataro<sup>78A,78C</sup>, S. Stansilau<sup>73</sup>, F. Stieler<sup>37</sup>, S. S. Su<sup>42</sup>, G. B. Sun<sup>80</sup>, G. X. Sun<sup>1</sup>, B.

H. Sun<sup>67</sup> , H. K. Sun<sup>1</sup> , J. F. Sun<sup>20</sup> , K. Sun<sup>64</sup> , L. Sun<sup>80</sup> , R. Sun<sup>75</sup> , S. S. Sun<sup>1,67</sup> , T. Sun<sup>54,e</sup> , W. Y. Sun<sup>53</sup> ,  
Y. C. Sun<sup>80</sup> , Y. H. Sun<sup>32</sup> , Y. J. Sun<sup>75,61</sup> , Y. Z. Sun<sup>1</sup> , Z. Q. Sun<sup>1,67</sup> , Z. T. Sun<sup>52</sup> , C. J. Tang<sup>57</sup> , G. Y. Tang<sup>1</sup> ,  
J. Tang<sup>62</sup> , J. J. Tang<sup>75,61</sup> , L. F. Tang<sup>41</sup> , Y. A. Tang<sup>80</sup> , L. Y. Tao<sup>76</sup> , M. Tat<sup>73</sup> , J. X. Teng<sup>75,61</sup> ,  
J. Y. Tian<sup>75,61</sup> , W. H. Tian<sup>62</sup> , Y. Tian<sup>33</sup> , Z. F. Tian<sup>80</sup> , I. Uman<sup>65B</sup> , B. Wang<sup>1</sup> , B. Wang<sup>62</sup> , Bo Wang<sup>75,61</sup> ,  
C. Wang<sup>40,j,k</sup> , C. Wang<sup>20</sup> , Cong Wang<sup>23</sup> , D. Y. Wang<sup>48,g</sup> , H. J. Wang<sup>40,j,k</sup> , J. Wang<sup>9</sup> , J. J. Wang<sup>80</sup> ,  
J. P. Wang<sup>52</sup> , K. Wang<sup>1,61</sup> , L. L. Wang<sup>1</sup> , L. W. Wang<sup>36</sup> , M. Wang<sup>52</sup> , M. Wang<sup>75,61</sup> , N. Y. Wang<sup>37</sup> ,  
S. Wang<sup>12,f</sup> , S. Wang<sup>40,j,k</sup> , T. Wang<sup>12,f</sup> , T. J. Wang<sup>45</sup> , W. Wang<sup>62</sup> , W. P. Wang<sup>37</sup> , X. Wang<sup>48,g</sup> ,  
X. F. Wang<sup>40,j,k</sup> , X. L. Wang<sup>12,f</sup> , X. N. Wang<sup>1,67</sup> , Xin Wang<sup>27,h</sup> , Y. Wang<sup>1</sup> , Y. D. Wang<sup>47</sup> ,  
Y. F. Wang<sup>1,8,67</sup> , Y. H. Wang<sup>40,j,k</sup> , Y. J. Wang<sup>75,61</sup> , Y. L. Wang<sup>20</sup> , Y. N. Wang<sup>47</sup> , Y. N. Wang<sup>80</sup> ,  
Yaqian Wang<sup>18</sup> , Yi Wang<sup>64</sup> , Yuan Wang<sup>18,33</sup> , Z. Wang<sup>1,61</sup> , Z. Wang<sup>45</sup> , Z. L. Wang<sup>2</sup> , Z. Q. Wang<sup>12,f</sup> ,  
Z. Y. Wang<sup>1,67</sup> , Ziyi Wang<sup>67</sup> , D. Wei<sup>45</sup> , D. H. Wei<sup>14</sup> , H. R. Wei<sup>45</sup> , F. Weidner<sup>72</sup> , S. P. Wen<sup>1</sup> , U. Wiedner<sup>3</sup> ,  
G. Wilkinson<sup>73</sup> , M. Wolke<sup>79</sup> , J. F. Wu<sup>1,8</sup> , L. H. Wu<sup>1</sup> , L. J. Wu<sup>1,67</sup> , L. J. Wu<sup>20</sup> , Lianjie Wu<sup>20</sup> , S. G. Wu<sup>1,67</sup> ,  
M. M. Wu<sup>67</sup> , X. Wu<sup>12,f</sup> , Y. J. Wu<sup>33</sup> , Z. Wu<sup>1,61</sup> , L. Xia<sup>75,61</sup> , B. H. Xiang<sup>1,67</sup> , D. Xiao<sup>40,j,k</sup> , G. Y. Xiao<sup>44</sup> ,  
H. Xiao<sup>76</sup> , Y. L. Xiao<sup>12,f</sup> , Z. J. Xiao<sup>43</sup> , C. Xie<sup>44</sup> , K. J. Xie<sup>1,67</sup> , Y. Xie<sup>52</sup> , Y. G. Xie<sup>1,61</sup> , Y. H. Xie<sup>6</sup> ,  
Z. P. Xie<sup>75,61</sup> , T. Y. Xing<sup>1,67</sup> , C. J. Xu<sup>62</sup> , G. F. Xu<sup>1</sup> , H. Y. Xu<sup>2</sup> , M. Xu<sup>75,61</sup> , Q. J. Xu<sup>17</sup> , Q. N. Xu<sup>32</sup> ,  
T. D. Xu<sup>76</sup> , X. P. Xu<sup>58</sup> , Y. Xu<sup>12,f</sup> , Y. C. Xu<sup>81</sup> , Z. S. Xu<sup>67</sup> , F. Yan<sup>24</sup> , L. Yan<sup>12,f</sup> , W. B. Yan<sup>75,61</sup> ,  
W. C. Yan<sup>84</sup> , W. H. Yan<sup>6</sup> , W. P. Yan<sup>20</sup> , X. Q. Yan<sup>1,67</sup> , H. J. Yang<sup>54,e</sup> , H. L. Yang<sup>36</sup> , H. X. Yang<sup>1</sup> ,  
J. H. Yang<sup>44</sup> , R. J. Yang<sup>20</sup> , Y. Yang<sup>12,f</sup> , Y. H. Yang<sup>44</sup> , Y. Q. Yang<sup>9</sup> , Y. Z. Yang<sup>20</sup> , Z. P. Yao<sup>52</sup> , M. Ye<sup>1,61</sup> ,  
M. H. Ye<sup>8,†</sup> , Z. J. Ye<sup>59,i</sup> , Junhao Yin<sup>45</sup> , Z. Y. You<sup>62</sup> , B. X. Yu<sup>1,61,67</sup> , C. X. Yu<sup>45</sup> , G. Yu<sup>13</sup> , J. S. Yu<sup>27,h</sup> ,  
L. W. Yu<sup>12,f</sup> , T. Yu<sup>76</sup> , X. D. Yu<sup>48,g</sup> , Y. C. Yu<sup>84</sup> , Y. C. Yu<sup>40</sup> , C. Z. Yuan<sup>1,67</sup> , H. Yuan<sup>1,67</sup> , J. Yuan<sup>36</sup> ,  
J. Yuan<sup>47</sup> , L. Yuan<sup>2</sup> , M. K. Yuan<sup>12,f</sup> , S. H. Yuan<sup>76</sup> , Y. Yuan<sup>1,67</sup> , C. X. Yue<sup>41</sup> , Ying Yue<sup>20</sup> , A. A. Zafar<sup>77</sup> ,  
F. R. Zeng<sup>52</sup> , S. H. Zeng<sup>66</sup> , X. Zeng<sup>12,f</sup> , Yujie Zeng<sup>62</sup> , Y. J. Zeng<sup>1,67</sup> , Y. C. Zhai<sup>52</sup> , Y. H. Zhan<sup>62</sup> ,  
Shunan Zhang<sup>73</sup> , B. L. Zhang<sup>1,67</sup> , B. X. Zhang<sup>1,†</sup> , D. H. Zhang<sup>45</sup> , G. Y. Zhang<sup>20</sup> , G. Y. Zhang<sup>1,67</sup> ,  
H. Zhang<sup>75,61</sup> , H. Zhang<sup>84</sup> , H. C. Zhang<sup>1,61,67</sup> , H. H. Zhang<sup>62</sup> , H. Q. Zhang<sup>1,61,67</sup> , H. R. Zhang<sup>75,61</sup> ,  
H. Y. Zhang<sup>1,61</sup> , J. Zhang<sup>62</sup> , J. J. Zhang<sup>55</sup> , J. L. Zhang<sup>21</sup> , J. Q. Zhang<sup>43</sup> , J. S. Zhang<sup>12,f</sup> ,  
J. W. Zhang<sup>1,61,67</sup> , J. X. Zhang<sup>40,j,k</sup> , J. Y. Zhang<sup>1</sup> , J. Z. Zhang<sup>1,67</sup> , Jianyu Zhang<sup>67</sup> , L. M. Zhang<sup>64</sup> ,  
Lei Zhang<sup>44</sup> , N. Zhang<sup>84</sup> , P. Zhang<sup>1,8</sup> , Q. Zhang<sup>20</sup> , Q. Y. Zhang<sup>36</sup> , R. Y. Zhang<sup>40,j,k</sup> , S. H. Zhang<sup>1,67</sup> ,  
Shulei Zhang<sup>27,h</sup> , X. M. Zhang<sup>1</sup> , X. Y. Zhang<sup>52</sup> , Y. Zhang<sup>1</sup> , Y. Zhang<sup>76</sup> , Y. T. Zhang<sup>84</sup> , Y. H. Zhang<sup>1,61</sup> ,  
Y. P. Zhang<sup>75,61</sup> , Z. D. Zhang<sup>1</sup> , Z. H. Zhang<sup>1</sup> , Z. L. Zhang<sup>36</sup> , Z. L. Zhang<sup>58</sup> , Z. X. Zhang<sup>20</sup> , Z. Y. Zhang<sup>80</sup> ,  
Z. Y. Zhang<sup>45</sup> , Z. Z. Zhang<sup>47</sup> , Zh. Zh. Zhang<sup>20</sup> , G. Zhao<sup>1</sup> , J. Y. Zhao<sup>1,67</sup> , J. Z. Zhao<sup>1,61</sup> , L. Zhao<sup>1</sup> ,  
L. Zhao<sup>75,61</sup> , M. G. Zhao<sup>45</sup> , S. J. Zhao<sup>84</sup> , Y. B. Zhao<sup>1,61</sup> , Y. L. Zhao<sup>58</sup> , Y. X. Zhao<sup>33,67</sup> , Z. G. Zhao<sup>75,61</sup> ,  
A. Zhemchugov<sup>38,a</sup> , B. Zheng<sup>76</sup> , B. M. Zheng<sup>36</sup> , J. P. Zheng<sup>1,61</sup> , W. J. Zheng<sup>1,67</sup> , X. R. Zheng<sup>20</sup> ,  
Y. H. Zheng<sup>67,o</sup> , B. Zhong<sup>43</sup> , C. Zhong<sup>20</sup> , H. Zhou<sup>37,52,n</sup> , J. Q. Zhou<sup>36</sup> , S. Zhou<sup>6</sup> , X. Zhou<sup>80</sup> , X. K. Zhou<sup>6</sup> ,  
X. R. Zhou<sup>75,61</sup> , X. Y. Zhou<sup>41</sup> , Y. X. Zhou<sup>81</sup> , Y. Z. Zhou<sup>12,f</sup> , A. N. Zhu<sup>67</sup> , J. Zhu<sup>45</sup> , K. Zhu<sup>1</sup> ,  
K. J. Zhu<sup>1,61,67</sup> , K. S. Zhu<sup>12,f</sup> , L. Zhu<sup>36</sup> , L. X. Zhu<sup>67</sup> , S. H. Zhu<sup>74</sup> , T. J. Zhu<sup>12,f</sup> , W. D. Zhu<sup>12,f</sup> ,  
W. J. Zhu<sup>1</sup> , W. Z. Zhu<sup>20</sup> , Y. C. Zhu<sup>75,61</sup> , Z. A. Zhu<sup>1,67</sup> , X. Y. Zhuang<sup>45</sup> , J. H. Zou<sup>1</sup> , J. Zu<sup>75,61</sup> 

(BESIII Collaboration)

<sup>1</sup> Institute of High Energy Physics, Beijing 100049, People's Republic of China

<sup>2</sup> Beihang University, Beijing 100191, People's Republic of China

<sup>3</sup> Bochum Ruhr-University, D-44780 Bochum, Germany

<sup>4</sup> Budker Institute of Nuclear Physics SB RAS (BINP), Novosibirsk 630090, Russia

<sup>5</sup> Carnegie Mellon University, Pittsburgh, Pennsylvania 15213, USA

<sup>6</sup> Central China Normal University, Wuhan 430079, People's Republic of China

<sup>7</sup> Central South University, Changsha 410083, People's Republic of China

<sup>8</sup> China Center of Advanced Science and Technology, Beijing 100190, People's Republic of China

<sup>9</sup> China University of Geosciences, Wuhan 430074, People's Republic of China

- <sup>26</sup> Hunan Normal University, Changsha 410081, People's Republic of China
- <sup>27</sup> Hunan University, Changsha 410082, People's Republic of China
- <sup>28</sup> Indian Institute of Technology Madras, Chennai 600036, India
- <sup>29</sup> Indiana University, Bloomington, Indiana 47405, USA
- <sup>30</sup> INFN Laboratori Nazionali di Frascati, (A)INFN Laboratori Nazionali di Frascati, I-00044, Frascati, Italy; (B)INFN Sezione di Perugia, I-06100, Perugia, Italy; (C)University of Perugia, I-06100, Perugia, Italy
- <sup>31</sup> INFN Sezione di Ferrara, (A)INFN Sezione di Ferrara, I-44122, Ferrara, Italy; (B)University of Ferrara, I-44122, Ferrara, Italy
- <sup>32</sup> Inner Mongolia University, Hohhot 010021, People's Republic of China
- <sup>33</sup> Institute of Modern Physics, Lanzhou 730000, People's Republic of China
- <sup>34</sup> Institute of Physics and Technology, Mongolian Academy of Sciences, Peace Avenue 54B, Ulaanbaatar 13330, Mongolia
- <sup>35</sup> Instituto de Alta Investigación, Universidad de Tarapacá, Casilla 7D, Arica 1000000, Chile
- <sup>36</sup> Jilin University, Changchun 130012, People's Republic of China
- <sup>37</sup> Johannes Gutenberg University of Mainz, Johann-Joachim-Becher-Weg 45, D-55099 Mainz, Germany
- <sup>38</sup> Joint Institute for Nuclear Research, 141980 Dubna, Moscow region, Russia
- <sup>39</sup> Justus-Liebig-Universität Giessen, II. Physikalisches Institut, Heinrich-Buff-Ring 16, D-35392 Giessen, Germany
- <sup>40</sup> Lanzhou University, Lanzhou 730000, People's Republic of China
- <sup>41</sup> Liaoning Normal University, Dalian 116029, People's Republic of China
- <sup>42</sup> Liaoning University, Shenyang 110036, People's Republic of China
- <sup>43</sup> Nanjing Normal University, Nanjing 210023, People's Republic of China
- <sup>44</sup> Nanjing University, Nanjing 210093, People's Republic of China
- <sup>45</sup> Nankai University, Tianjin 300071, People's Republic of China
- <sup>46</sup> National Centre for Nuclear Research, Warsaw 02-093, Poland
- <sup>47</sup> North China Electric Power University, Beijing 102206, People's Republic of China
- <sup>48</sup> Peking University, Beijing 100871, People's Republic of China
- <sup>49</sup> Qufu Normal University, Qufu 273165, People's Republic of China
- <sup>50</sup> Renmin University of China, Beijing 100872, People's Republic of China
- <sup>51</sup> Shandong Normal University, Jinan 250014, People's Republic of China
- <sup>52</sup> Shandong University, Jinan 250100, People's Republic of China
- <sup>53</sup> Shandong University of Technology, Zibo 255000, People's Republic of China
- <sup>54</sup> Shanghai Jiao Tong University, Shanghai 200240, People's Republic of China
- <sup>55</sup> Shanxi Normal University, Linfen 041004, People's Republic of China
- <sup>56</sup> Shanxi University, Taiyuan 030006, People's Republic of China
- <sup>57</sup> Sichuan University, Chengdu 610064, People's Republic of China
- <sup>58</sup> Soochow University, Suzhou 215006, People's Republic of China
- <sup>59</sup> South China Normal University, Guangzhou 510006, People's Republic of China
- <sup>60</sup> Southeast University, Nanjing 211100, People's Republic of China
- <sup>61</sup> State Key Laboratory of Particle Detection and Electronics, Beijing 100049, Hefei 230026, People's Republic of China
- <sup>62</sup> Sun Yat-Sen University, Guangzhou 510275, People's Republic of China
- <sup>63</sup> Suranaree University of Technology, University Avenue 111, Nakhon Ratchasima 30000, Thailand
- <sup>64</sup> Tsinghua University, Beijing 100084, People's Republic of China
- <sup>65</sup> Turkish Accelerator Center Particle Factory Group, (A)Istinye University, 34010, Istanbul, Turkey; (B)Near East University, Nicosia, North Cyprus, 99138, Mersin 10, Turkey
- <sup>66</sup> University of Bristol, H H Wills Physics Laboratory, Tyndall Avenue, Bristol, BS8 1TL, UK
- <sup>67</sup> University of Chinese Academy of Sciences, Beijing 100049, People's Republic of China
- <sup>68</sup> University of Groningen, NL-9747 AA Groningen, The Netherlands
- <sup>69</sup> University of Hawaii, Honolulu, Hawaii 96822, USA
- <sup>70</sup> University of Jinan, Jinan 250022, People's Republic of China
- <sup>71</sup> University of Manchester, Oxford Road, Manchester, M13 9PL, United Kingdom
- <sup>72</sup> University of Muenster, Wilhelm-Klemm-Strasse 9, 48149 Muenster, Germany
- <sup>73</sup> University of Oxford, Keble Road, Oxford OX13RH, United Kingdom
- <sup>74</sup> University of Science and Technology Liaoning, Anshan 114051, People's Republic of China
- <sup>75</sup> University of Science and Technology of China, Hefei 230026, People's Republic of China
- <sup>76</sup> University of South China, Hengyang 421001, People's Republic of China
- <sup>77</sup> University of the Punjab, Lahore-54590, Pakistan
- <sup>78</sup> University of Turin and INFN, (A)University of Turin, I-10125, Turin, Italy; (B)University of Eastern Piedmont, I-15121, Alessandria, Italy; (C)INFN, I-10125, Turin, Italy
- <sup>79</sup> Uppsala University, Box 516, SE-75120 Uppsala, Sweden
- <sup>80</sup> Wuhan University, Wuhan 430072, People's Republic of China
- <sup>81</sup> Yantai University, Yantai 264005, People's Republic of China
- <sup>82</sup> Yunnan University, Kunming 650500, People's Republic of China
- <sup>83</sup> Zhejiang University, Hangzhou 310027, People's Republic of China
- <sup>84</sup> Zhengzhou University, Zhengzhou 450001, People's Republic of China

† Deceased

<sup>a</sup> Also at the Moscow Institute of Physics and Technology, Moscow 141700, Russia

<sup>b</sup> Also at the Novosibirsk State University, Novosibirsk, 630090, Russia

<sup>c</sup> Also at the NRC "Kurchatov Institute", PNPI, 188300, Gatchina, Russia

<sup>d</sup> Also at Goethe University Frankfurt, 60323 Frankfurt am Main, Germany

<sup>e</sup> Also at Key Laboratory for Particle Physics, Astrophysics and Cosmology, Ministry of Education; Shanghai Key Laboratory for Particle Physics and Cosmology; Institute of Nuclear and Particle Physics, Shanghai 200240, People's Republic of China

<sup>f</sup> Also at Key Laboratory of Nuclear Physics and Ion-beam Application (MOE) and Institute of Modern Physics, Fudan University, Shanghai 200443, People's Republic of China

<sup>g</sup> Also at State Key Laboratory of Nuclear Physics and Technology, Peking University, Beijing 100871, People's Republic of China

<sup>h</sup> Also at School of Physics and Electronics, Hunan University, Changsha 410082, China

<sup>i</sup> Also at Guangdong Provincial Key Laboratory of Nuclear Science, Institute of Quantum Matter, South China Normal University, Guangzhou 510006, China

<sup>j</sup> Also at MOE Frontiers Science Center for Rare Isotopes, Lanzhou University, Lanzhou 730000, People's Republic of China

<sup>k</sup> Also at Lanzhou Center for Theoretical Physics, Lanzhou University, Lanzhou 730000, People's Republic of China

<sup>l</sup> Also at the Department of Mathematical Sciences, IBA, Karachi 75270, Pakistan

<sup>m</sup> Also at Ecole Polytechnique Federale de Lausanne (EPFL), CH-1015 Lausanne, Switzerland

<sup>n</sup> Also at Helmholtz Institute Mainz, Staudinger Weg 18, D-55099 Mainz, Germany

<sup>o</sup> Also at Hangzhou Institute for Advanced Study, University of Chinese Academy of Sciences, Hangzhou 310024, China

<sup>p</sup> Currently at Silesian University in Katowice, Chorzow, 41-500, Poland

By analyzing  $e^+e^-$  collision data corresponding to an integrated luminosity of  $7.33 \text{ fb}^{-1}$  collected with the BESIII detector at center-of-mass energies ranging from 4.128 to 4.226 GeV, we report the observations of the hadronic decays  $D_s^+ \rightarrow K_S^0 K_S^0 \pi^+ \pi^0$  and  $D_s^+ \rightarrow K_S^0 K^+ \pi^0 \pi^0$ . Their decay branching fractions are determined to be  $\mathcal{B}(D_s^+ \rightarrow K_S^0 K_S^0 \pi^+ \pi^0) = (4.08 \pm 0.46_{\text{stat}} \pm 0.45_{\text{syst}}) \times 10^{-3}$  and  $\mathcal{B}(D_s^+ \rightarrow K_S^0 K^+ \pi^0 \pi^0) = (3.32 \pm 0.64_{\text{stat}} \pm 0.31_{\text{syst}}) \times 10^{-3}$ , where the first uncertainties are statistical and the second are systematic.

## I. INTRODUCTION

Experimental studies of hadronic  $D_s^+$  decays offer important information to improve the understanding of  $CP$  violation and quark  $SU(3)$  symmetry breaking effects in the charm sector [1, 2]. Four-body heavy hadron weak decays provide a rich phenomenology for improving our understanding of QCD in hadronization, including differential distributions [3] and triple-product correlations [4], and to test *e.g.* the factorization approach [5]. Intensive studies of four-body  $D_s^+$  decays benefit the understanding the  $D_s^+$  decay mechanisms. To date, the hadronic decays  $D_s^+ \rightarrow K^+ K^- \pi^+ \pi^0$  [6],  $D_s^+ \rightarrow K_S^0 K^- \pi^+ \pi^+$  [7], and  $D_s^+ \rightarrow K_S^0 K^+ \pi^+ \pi^-$  have been well investigated in experiments, but no information about  $D_s^+ \rightarrow K_S^0 K_S^0 \pi^+ \pi^0$  and  $D_s^+ \rightarrow K_S^0 K^+ \pi^0 \pi^0$  has been reported [8].

In this article, we report the observation of the decays  $D_s^+ \rightarrow K_S^0 K_S^0 \pi^+ \pi^0$  and  $D_s^+ \rightarrow K_S^0 K^+ \pi^0 \pi^0$ , and determine their decay branching fractions, by analyzing  $e^+e^-$  collision data corresponding to an integrated luminosity of  $7.33 \text{ fb}^{-1}$  collected with the BESIII detector at center-of-mass energies ( $E_{\text{cm}}$ ) between 4.128 and 4.226 GeV. Charge conjugated decays,  $D_s^- \rightarrow K_S^0 K_S^0 \pi^- \pi^0$  and  $D_s^- \rightarrow K_S^0 K^- \pi^0 \pi^0$ , are always included throughout this paper.

## II. BESIII DETECTOR AND MONTE CARLO SIMULATION

The BESIII detector [9] records symmetric  $e^+e^-$  collisions provided by the BEPCII storage ring [10] in the center-of-mass energy range from 1.84 to 4.95 GeV, with a peak luminosity of  $1.1 \times 10^{33} \text{ cm}^{-2}\text{s}^{-1}$  achieved at  $\sqrt{s} = 3.773 \text{ GeV}$ . The cylindrical core of the BESIII detector covers 93% of the full solid angle and consists of a helium-based multilayer drift chamber (MDC), a time-of-flight system (TOF), and a CsI(Tl) electromagnetic calorimeter (EMC), which are all enclosed in a superconducting solenoidal magnet providing a 1.0 T magnetic field. The solenoid is supported by an octagonal flux-return yoke with resistive plate counter muon identification modules interleaved with steel. The charged-particle momentum resolution at 1 GeV/c is 0.5%, and the specific ionisation energy loss,  $dE/dx$ , resolution is 6% for electrons from Bhabha scattering. The EMC measures photon energies with a resolution of 2.5% (5%) at 1 GeV in the barrel (end-cap) region. The time resolution in the plastic scintillator TOF barrel region is 68 ps, while that in the end-cap region was 110 ps. The end-cap TOF system was upgraded in 2015 using multigap resistive plate chamber technology, providing a time resolution of 60 ps, which benefits 63% of the data used in this analysis [11]. Luminosities [12] at each energy are given in Table 1.

Monte Carlo (MC) simulated data samples produced with a GEANT4-based [13] software package, which includes the geometric description of the BESIII detector

and the detector response, are used to determine detection efficiencies and to estimate backgrounds. The simulation models the beam energy spread and initial state radiation (ISR) in the  $e^+e^-$  annihilations with the generator KKMC [14]. The inclusive MC sample includes the production of  $D\bar{D}$  pairs (including quantum coherence for the neutral  $D$  channels), the non- $D\bar{D}$  decays of the  $\psi(3770)$ , the ISR production of the  $J/\psi$  and  $\psi(3686)$  states, and the continuum processes incorporated in KKMC [14]. All particle decays are modeled with EVTGEN [15] using branching fractions either taken from the Particle Data Group (PDG) [8], when available, or otherwise estimated with LUNDCHARM [16]. Final state radiation from charged final state particles is incorporated using the PHOTOS package [17]. The signal MC samples of  $D_s^+ \rightarrow K_S^0 K_S^0 \pi^+ \pi^0$  and  $D_s^+ \rightarrow K_S^0 K^+ \pi^0 \pi^0$  are generated with mixed subdecays with branching fractions quoted from the PDG [8].

### III. MEASUREMENT METHOD

In  $e^+e^-$  collisions taken at  $E_{\text{cm}}$  between 4.128 and 4.226 GeV, the  $D_s^\pm$  mesons are produced mainly via the process  $e^+e^- \rightarrow D_s^{*\pm} D_s^\mp \rightarrow \gamma(\pi^0) D_s^+ D_s^-$ . We perform this analysis by using the double-tag (DT) method [18, 19], which was first developed by the MARKIII Collaboration. The  $D_s^-$  meson, which is fully reconstructed via one of sixteen hadronic decay modes, is referred to as a single-tag (ST)  $D_s^-$  meson. The event, in which the transition  $\gamma(\pi^0)$  from  $D_s^{*+}$  and the signal decay can be successfully selected in the presence of ST  $D_s^-$  meson, is called a DT event. For a specific ST mode  $i$ , the ST and DT yields observed in data are given by

$$N_{\text{ST}}^i = 2N_{D_s^+ D_s^{*-}} \mathcal{B}_{\text{ST}}^i \epsilon_{\text{ST}}^i, \quad (1)$$

and

$$N_{\text{DT}}^i = 2N_{D_s^+ D_s^{*-}} \mathcal{B}_{\text{ST}}^i \mathcal{B}_{\text{sig}} \epsilon_{\text{ST}, D_s^+ \rightarrow \text{sig}}^i, \quad (2)$$

where  $N_{D_s^+ D_s^{*-}}$  is the number of  $D_s^+ D_s^{*-}$  pairs produced in data,  $\mathcal{B}_{\text{ST}}^i$  is the branching fraction for the ST mode  $i$ ,  $\mathcal{B}_{\text{sig}}$  is the branching fraction for  $D_s^+ \rightarrow K_S^0 K_S^0 \pi^+ \pi^0$  or  $D_s^+ \rightarrow K_S^0 K^+ \pi^0 \pi^0$ ,  $\epsilon_{\text{ST}}^i$  is the efficiency of reconstructing the ST mode  $i$  (called the ST efficiency), and  $\epsilon_{\text{ST}, D_s^+ \rightarrow \text{sig}}^i$  is the efficiency of simultaneously finding the ST mode  $i$  and the  $D_s^+ \rightarrow \text{sig}$  decay (called the DT efficiency). The branching fractions of  $D_s^{*-} \rightarrow \gamma(\pi^0) D_s^-$  are included in the DT efficiency. Based on these two equations, the branching fraction of the signal decay is determined as

$$\mathcal{B}_{\text{sig}} = \frac{N_{\text{DT}}}{N_{\text{ST}}^{\text{tot}} \cdot \epsilon_{\gamma(\pi^0)\text{sig}} \cdot (B_{K_S^0})^k (B_{\pi^0})^j}, \quad (3)$$

where  $N_{\text{DT}}$  and  $N_{\text{ST}}^{\text{tot}}$  are the numbers of the DT events and the ST  $D_s^-$  mesons in data summing over tag modes,

respectively;  $\epsilon_{\gamma(\pi^0)\text{sig}} = \sum_i \frac{N_{\text{ST}}^i \cdot \epsilon_{\gamma(\pi^0)\text{sig}}^i}{N_{\text{ST}}^{\text{tot}}}$  is the efficiency of detecting the signal decay in the presence of the ST  $D_s^-$  mesons, which is averaged by the ST  $D_s^-$  yields  $N_{\text{ST}}^i$  for different tag modes;  $B_{K_S^0}$  ( $B_{\pi^0}$ ) is the branching fraction of  $K_S^0 \rightarrow \pi^+ \pi^-$  ( $\pi^0 \rightarrow \gamma\gamma$ ) from PDG [8];  $k$  ( $j$ ) is the number of  $K_S^0$  ( $\pi^0$ ) mesons in the final state of DT side.

### IV. SINGLE-TAG CANDIDATES

The ST  $D_s^-$  candidates are reconstructed from sixteen hadronic decay modes of  $K^+ K^- \pi^-$ ,  $K^+ K^- \pi^- \pi^0$ ,  $\pi^- \pi^+ \pi^-$ ,  $K_S^0 K^-$ ,  $K_S^0 K^- \pi^0$ ,  $K^- \pi^+ \pi^-$ ,  $K_S^0 K_S^0 \pi^-$ ,  $K_S^0 K^+ \pi^- \pi^-$ ,  $K_S^0 K^- \pi^+ \pi^-$ ,  $\eta_{\gamma\gamma} \pi^-$ ,  $\eta_{\pi^+ \pi^- \pi^0} \pi^-$ ,  $\eta'_{\gamma\rho} \pi^-$ ,  $\eta'_{\eta\pi^+ \pi^-} \pi^-$ ,  $\eta_{\gamma\gamma} \rho^-$ ,  $\eta_{\pi^+ \pi^- \pi^0} \rho^-$ , and  $\eta_{\gamma\gamma} \pi^+ \pi^- \pi^-$ . Throughout this paper,  $\rho$  denotes  $\rho(770)$  and the subscripts of  $\eta^{(\prime)}$  denote individual decay modes that are used to reconstruct the  $\eta^{(\prime)}$  candidates.

All charged tracks, except for those from  $K_S^0$ , must be from a region near the interaction point defined as  $|V_{xy}| < 1$  cm,  $|V_z| < 10$  cm, and  $|\cos\theta| < 0.93$ , where  $|V_{xy}|$  and  $|V_z|$  are distances of the closest approach in the transverse plane and along the MDC axis, respectively, and  $\theta$  is the polar angle with respect to the MDC axis. We identify charged particles by using the combined  $dE/dx$  and TOF information, based on which the confidence levels for pion and kaon hypotheses are calculated. The charged tracks with confidence level for the pion (kaon) hypothesis greater than that for the kaon (pion) hypothesis are identified as pion (kaon) candidates.

The  $K_S^0$  candidates are formed with the decays  $K_S^0 \rightarrow \pi^+ \pi^-$ . The two charged pions must satisfy the requirements  $|V_z| < 20$  cm and  $|\cos\theta| < 0.93$ . The tracks are assumed to be  $\pi^+ \pi^-$  without any particle identification (PID) requirement, and the invariant mass of the  $\pi^+ \pi^-$  combination has to be within (0.486, 0.510) MeV/ $c^2$ . The two charged tracks are constrained to originate from a common vertex, which is required to be away from the interaction point by a flight distance of at least twice the vertex resolution.

Photon candidates are selected by using the isolated showers measured in the EMC. To suppress backgrounds from electronic noise or bremsstrahlung, any candidate shower is required to start within [0, 700] ns from the event start time. The energy of each shower in the barrel EMC region [9] is required to be greater than 25 MeV; while that in the end-cap EMC region must be larger than 50 MeV. To reject the backgrounds associated with charged tracks, the opening angle between the shower and the extrapolated direction on the EMC of the nearest charged track is required to be larger than  $10^\circ$ .

Candidates for  $\pi^0$  and  $\eta_{\gamma\gamma}$  are formed from the  $\gamma\gamma$  pairs with invariant masses in the ranges of (0.115, 0.150) and (0.500, 0.570) GeV/ $c^2$ , respectively. To improve momentum resolution, a one-constraint (1C) kinematic fit on the selected  $\gamma\gamma$  pair con-

Table 1. The integrated luminosity and  $M_{\text{BC}}$  requirement for each energy ( $E_{\text{cm}}$ ) point.

$E_{\text{cm}}$ (GeV)	Luminosity ( $\text{pb}^{-1}$ )	$M_{\text{BC}}$ ( $\text{GeV}/c^2$ )
4.128	401.5	[2.010, 2.061]
4.157	408.7	[2.010, 2.070]
4.178	3189.0	[2.010, 2.073]
4.189	569.8	[2.010, 2.076]
4.199	526.0	[2.010, 2.079]
4.209	571.7	[2.010, 2.082]
4.219	568.7	[2.010, 2.085]
4.226	1091.7	[2.010, 2.088]

strains their invariant mass to the known  $\pi^0$  or  $\eta$  mass [8]. Candidates for  $\rho^{+(0)}$ ,  $\eta_{\pi^0\pi^+\pi^-}$ ,  $\eta'_{\eta\pi^+\pi^-}$ , and  $\eta'_{\gamma\rho^0}$  are formed from the  $\pi^+\pi^0(-)$ ,  $\pi^0\pi^+\pi^-$ ,  $\eta\pi^+\pi^-$ , and  $\gamma\rho^0$  combinations with invariant masses in the ranges of (0.570, 0.970)  $\text{GeV}/c^2$ , (0.530, 0.570)  $\text{GeV}/c^2$ , (0.946, 0.970)  $\text{GeV}/c^2$  and (0.940, 0.976)  $\text{GeV}/c^2$ , respectively. In addition, the minimum energy of the  $\gamma$  candidate decaying from  $\eta'_{\gamma\rho^0}$  must be larger than 0.1 GeV.

To veto the soft pions from  $D^{*+}$  decays, the momentum of any pion which is not from  $K_S^0$ ,  $\eta$ , or  $\eta'$  is required to be greater than 0.1  $\text{GeV}/c$ . To reject the peaking background from  $D_s^- \rightarrow K_S^0\pi^-$  in the selection of the tag mode  $D_s^- \rightarrow \pi^-\pi^+\pi^-$ , the invariant mass of any  $\pi^+\pi^-$  combination must be outside the range of (0.468, 0.528)  $\text{GeV}/c^2$ .

To suppress the backgrounds from the non- $D_s^\pm D_s^{*\mp}$  processes, we define a kinematic variable, beam-constrained mass of the ST  $D_s^-$  candidate,

$$M_{\text{BC}} \equiv \sqrt{E_{\text{beam}}^2/4c^4 - |\vec{p}_{\text{tag}}|^2/c^2} \quad (4)$$

where  $E_{\text{beam}}$  is the beam energy and  $\vec{p}_{\text{tag}}$  is the momentum of the ST  $D_s^-$  candidate in the rest frame of the  $e^+e^-$  system. For each candidate, the  $M_{\text{BC}}$  must satisfy the selection criteria listed in Table 1. Figure 1 shows the  $M_{\text{BC}}$  distribution of the ST candidates at 4.178 GeV. These requirements retain most  $D_s^-$  and  $D_s^+$  mesons from  $e^+e^- \rightarrow D_s^{*\mp} D_s^\pm$ .

If there are multiple candidates present per tag mode per charge, only the one with the  $D_s^-$  recoil mass

$$M_{\text{rec}} \equiv \sqrt{\left(E_{\text{cm}} - \sqrt{|\vec{p}_{\text{tag}}|^2 + m_{D_s^\pm}^2}\right)^2/c^4 - |\vec{p}_{\text{tag}}|^2/c^2} \quad (5)$$

closest to the known  $D_s^{*-}$  mass [8] is retained. Here,  $m_{D_s^\pm}$  is the nominal  $D_s^\pm$  mass [8]. The distributions of the invariant masses ( $M_{\text{tag}}$ ) of the accepted candidates for different tag modes are shown in Fig. 2. For each tag mode, the yield of ST  $D_s^-$  mesons is obtained from a fit to the individual  $M_{\text{tag}}$  distribution. In the fit, the signal is modeled by the simulated shape convolved with a Gaussian function to take into account the resolution

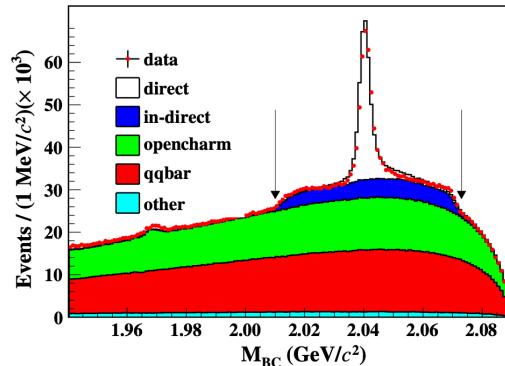


Fig. 1. Distributions of  $M_{\text{BC}}$  of the ST  $D_s^-$  candidates in data and inclusive MC samples at 4.178 GeV. The candidates between the two black arrows are retained for further analysis. The colored histograms represent various  $e^+e^-$  annihilation processes. These histograms are estimated with inclusive MC samples mentioned in Sec. II. The white (direct) histogram corresponds to events where the ST  $D_s^-$  candidate is produced directly from the  $e^+e^-$  annihilation, while the blue (in-direct) histogram represents events where the ST  $D_s^-$  candidate originates from the  $D_s^*$  decays. The green (opencharm) and red (qqbar) histograms are the backgrounds caused by  $e^+e^- \rightarrow D^{(*)}\bar{D}^{(*)}$  ( $D = D^+, D^0, D_s^+$ ) and  $e^+e^- \rightarrow q\bar{q}$  processes, respectively. The other (Cyan) histogram includes all other miscellaneous, such as the ISR production of  $J/\psi$  and  $\psi(3686)$ , etc.

difference between data and simulation. For the tag mode  $D_s^- \rightarrow K_S^0 K^-$ , the shape of the  $D_s^- \rightarrow K_S^0\pi^-$  peaking background is described by its simulated shape convolved with the same Gaussian resolution function that is smeared for the signal shape; while the size of this background is a free parameter in the fit. The combinatorial background is described by a first to third order Chebychev function, which has been validated with the inclusive MC sample. Figure 2 shows the results of the fits to the accepted ST  $D_s^-$  candidates from data combined from all energy points. In each plot, the pair of blue arrows indicates the chosen  $M_{\text{tag}}$  signal regions. Candidates in the  $M_{\text{tag}}$  signal regions are kept for further analysis. By studying the inclusive MC sample, we find that the process  $e^+e^- \rightarrow (\gamma_{\text{ISR}})D_s^+ D_s^-$  contributes about (0.7-1.1)% for the fitted yields of ST  $D_s^-$  mesons for different tag modes. For the fitted yields of the ST  $D_s^-$  mesons in data and the ST efficiencies, these backgrounds have been subtracted away based on inclusive MC simulation. The  $M_{\text{tag}}$  requirements, the yields of ST  $D_s^-$  mesons ( $N_{\text{tag}}$ ) for different tag modes and the ST efficiencies ( $\epsilon_{\text{tag}}$ ) are summarized in the second and third columns of Table 2, respectively. In this table, the shown yields of ST  $D_s^-$  mesons have been summed over all energy points, and the shown efficiencies of detecting ST  $D_s^-$  mesons are determined by averaging those by the corresponding yields of ST  $D_s^-$  mesons in

data at different energy points.

## V. DOUBLE-TAG CANDIDATES

In the side recoiling against the tagged  $D_s^-$  candidate, the transition photon or  $\pi^0$  and the signal  $D_s^+$  decay candidates are selected. We define the energy difference  $\Delta E \equiv E_{\text{cm}} - E_{\text{tag}} - E_{\gamma(\pi^0)D_s^-}^{\text{rec}} - E_{\gamma(\pi^0)}$ , where  $E_{\gamma(\pi^0)D_s^-}^{\text{rec}} \equiv \sqrt{|\vec{p}_{\gamma(\pi^0)} - \vec{p}_{\text{tag}}|^2 + m_{D_s^-}^2}$ ,  $E_i$  and  $\vec{p}_i$  [ $i = \gamma(\pi^0)$  or tag] are the energy and momentum of  $\gamma(\pi^0)$  or the tagged  $D_s^-$ , respectively. In this procedure, we loop over all unused  $\gamma$  or  $\pi^0$  candidates and retain the one with the minimum  $|\Delta E|$  for further analysis.

In the selection of the signal candidates, the selection criteria of  $\gamma$ ,  $\pi^0$ ,  $\pi^+$ ,  $K^+$ , and  $K_S^0$  are the same as those for tag side. For the  $D_s^+ \rightarrow K_S^0 K_S^0 \pi^+ \pi^0$  ( $D_s^+ \rightarrow K_S^0 K^+ \pi^0 \pi^0$ ) signal mode, if there are more than two (one)  $K_S^0$  candidates, those with the longest two (one) decay lengths are retained; if there are more than one (two)  $\pi^0$  candidate, those with one (two) minimum  $\chi_{1C}^2$  of the 1C kinematic fit for  $\pi^0 \rightarrow \gamma\gamma$  are kept.

Figure 3 shows the  $M_{\text{sig}}$  distributions of the accepted candidate events. Unbinned maximum likelihood fits are performed on these distributions. There is a peaking background caused by  $D_s^+ \rightarrow \rho^+ \phi$  for the signal decay  $D_s^+ \rightarrow K_S^0 K_S^0 \pi^+ \pi^0$ . In the fits, the signal, the peaking background and other background shapes are modeled by the simulated shapes obtained from the signal MC events and the inclusive MC sample, respectively. The peaking background yield is fixed according to MC simulation, while the signal and other background yields are set as free parameters. The significance of  $D_s^+ \rightarrow K_S^0 K_S^0 \pi^+ \pi^0$  ( $D_s^+ \rightarrow K_S^0 K^+ \pi^0 \pi^0$ ) is estimated to be  $8.3\sigma$  ( $5.1\sigma$ ), by comparing the difference in the likelihoods with and without involving the signal component in the fits, after taking into account the change of the number of degrees of freedom and the systematic uncertainties. In addition, we have also examined the  $M_{\text{sig}}$  distribution of events in the  $K_S^0$  sideband ( $0.02 < |M_{\pi^+\pi^-} - M_{K_S^0}| < 0.044 \text{ GeV}/c^2$ ) of data and find that they are negligible for both two decays.

The detection efficiencies are estimated to be  $(5.94 \pm 0.01)\%$  and  $(4.49 \pm 0.01)\%$  for  $D_s^+ \rightarrow K_S^0 K_S^0 \pi^+ \pi^0$  and  $D_s^+ \rightarrow K_S^0 K^+ \pi^0 \pi^0$ , respectively. Figures 4 and 5 show the comparisons of the invariant masses of two-body daughter particles of the accepted candidates for  $D_s^+ \rightarrow K_S^0 K_S^0 \pi^+ \pi^0$  and  $D_s^+ \rightarrow K_S^0 K^+ \pi^0 \pi^0$ , respectively. Good consistency between data and MC simulation ensures the reliability of the detection efficiencies.

With the known ST yield, the obtained signal yields and the corresponding signal efficiencies, we obtain the branching fractions of these decays, as listed in Table 3.

## VI. SYSTEMATIC UNCERTAINTY

The systematic uncertainties in the branching fraction measurements are discussed below. The uncertainty of the total ST yield,  $N_{\text{ST}}^{\text{tot}}$ , has been assigned as 0.5% according to Ref. [20]. The uncertainties from tracking and PID of  $\pi^+$  or  $K^+$  and  $\pi^0$  reconstruction are estimated by using the control samples of  $e^+e^- \rightarrow K^+K^-\pi^+\pi^-(\pi^0)$  and  $e^+e^- \rightarrow 2(\pi^+\pi^-)(\pi^0)$ . The systematic uncertainties of tracking (PID) efficiencies are assigned as 1.0% (1.0%) per  $\pi^+$  or  $K^+$ . The photon selection efficiency was previously studied with the  $J/\psi \rightarrow \pi^+\pi^-\pi^0$  decays. The systematic uncertainty in the transition  $\gamma(\pi^0)$  reconstruction is assigned as 1.0% [21]. The  $\pi^0$  reconstruction efficiencies include photon selection,  $\pi^0$  mass window, and 1C kinematic fit. The difference in efficiencies between data and MC simulation, 2.0% per  $\pi^0$ , is assigned as the systematic uncertainty [22].

The systematic uncertainty due to the selection of the best transition  $\gamma/\pi^0$  with the least  $|\Delta E|$  has also been studied in Ref. [23]. The systematic uncertainty from the selection of the transition  $\gamma(\pi^0)$  from  $D_s^{*+}$  with the least  $|\Delta E|$  method is estimated by using the control samples of  $D_s^+ \rightarrow K^+K^-\pi^+$  and  $D_s^+ \rightarrow \eta\pi^0\pi^+$ . The difference of the efficiencies of selecting the transition  $\gamma(\pi^0)$  candidates between data and MC simulation is taken as the corresponding systematic uncertainty, which is 0.4%.

The efficiencies of  $K_S^0$  reconstruction, including the tracking efficiencies of the  $\pi^+\pi^-$  pair, decay length requirement, mass window requirement, vertex fit and second vertex fit, are studied using the control samples of  $J/\psi \rightarrow K_S^0 K^\mp \pi^\pm$  and  $J/\psi \rightarrow \phi K_S^0 K^\mp \pi^\pm$ . The systematic uncertainty is assigned as the difference of efficiencies between data and MC simulation, which is 1.5% per  $K_S^0$  [24].

The uncertainties in  $M_{\text{sig}}$  fit are estimated by comparing the nominal signal yields with the ones measured by changing the alternative signal and background shapes. The alternative signal shapes are obtained from the inclusive MC sample. The alternative background shapes are obtained by varying the relative fraction of  $q\bar{q}$  background component in the nominal background shape derived from the inclusive MC sample by  $\pm 30\%$  [25, 26]. The changes of the fitted signal yields are assigned as the systematic uncertainties.

The systematic uncertainty of MC generator is estimated by using alternative signal MC samples. For  $D_s^+ \rightarrow K_S^0 K_S^0 \pi^+ \pi^0$ , the known branching fractions of different sub-resonant decays are varied by  $\pm 1\sigma$ . For  $D_s^+ \rightarrow K_S^0 K^+ \pi^0 \pi^0$ , the average signal efficiency for different sub-resonant decays is examined. The maximum changes of the signal efficiencies, 4.9% and 4.9%, are assigned as the systematic uncertainties for  $D_s^+ \rightarrow K_S^0 K_S^0 \pi^+ \pi^0$  and  $D_s^+ \rightarrow K_S^0 K^+ \pi^0 \pi^0$ , respectively.

The uncertainties in the quoted branching fractions of  $\pi^0 \rightarrow \gamma\gamma$  and  $K_S^0 \rightarrow \pi^+\pi^-$  are 0.03% and 0.07%. Varying

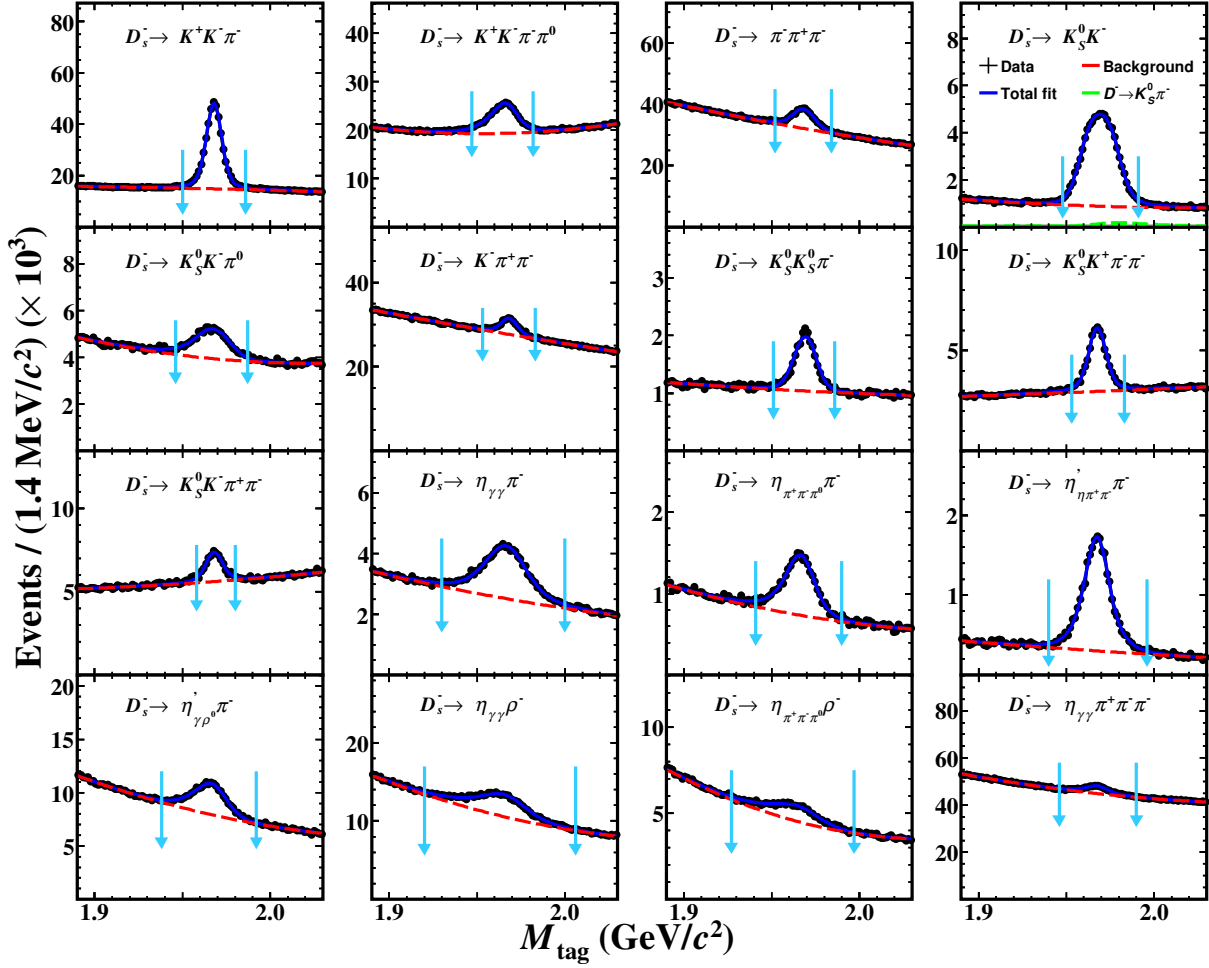


Fig. 2. Fits to the  $M_{\text{tag}}$  distributions of the accepted ST  $D_s^-$  candidates for different tag modes. The points with error bars are data summed over all energy points, the blue solid curves are the best fit results, and the red dashed curves are the fitted background shapes. For the  $D_s^- \rightarrow K_S^0 K^-$  tag mode, the green curve is the  $D^- \rightarrow K_S^0 \pi^-$  peaking background. The pair of light blue arrows denotes the  $M_{\text{tag}}$  signal regions.

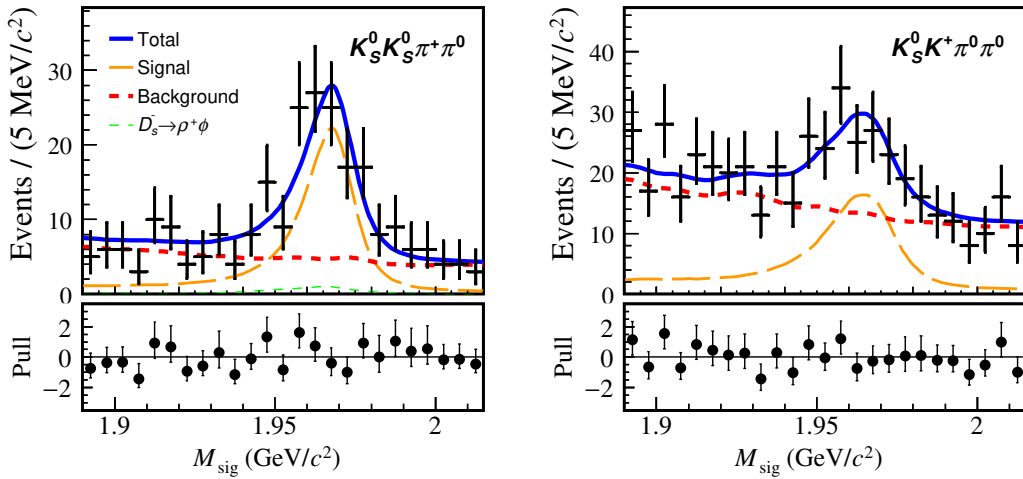


Fig. 3. Fits to the  $M_{\text{sig}}$  distributions of the accepted DT candidates. The points with error bars are data. The blue solid curves are the fit results. The yellow and red dashed curves are the fitted signals and combinatorial background, respectively. The green dashed curve represents the background bump caused by  $D_s^+ \rightarrow \rho^+ \phi$ .

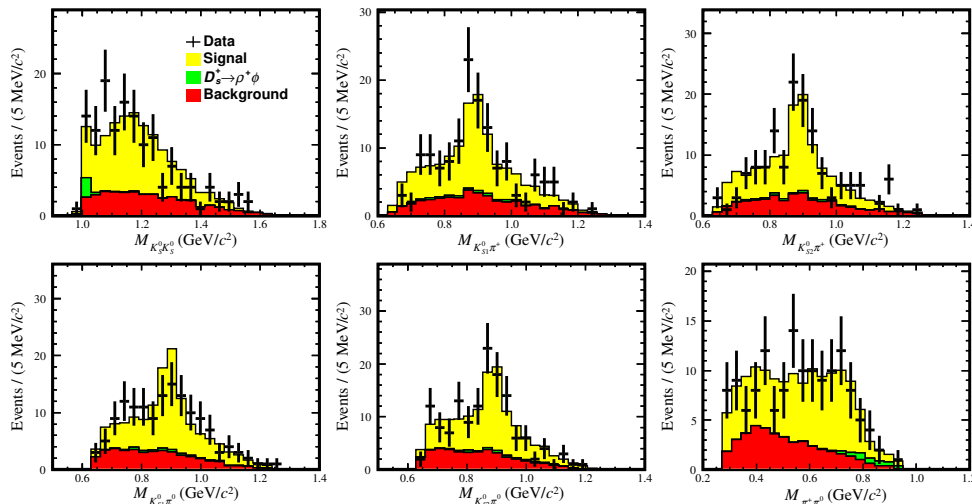


Fig. 4. Comparisons of  $M_{KK}$ ,  $M_{K\pi}$ , and  $M_{\pi\pi}$  for  $D_s^+ \rightarrow K_S^0 K_S^0 \pi^+ \pi^0$ . The points with error bars are data, the yellow filled histograms are signal, the green histogram represents the peaking background from  $D_s^+ \rightarrow \rho^+ \phi$ , and the red filled histograms are simulated backgrounds from the inclusive MC sample. Events have been further required to satisfy  $1.943 < M_{\text{sig}} < 1.983 \text{ GeV}/c^2$ .

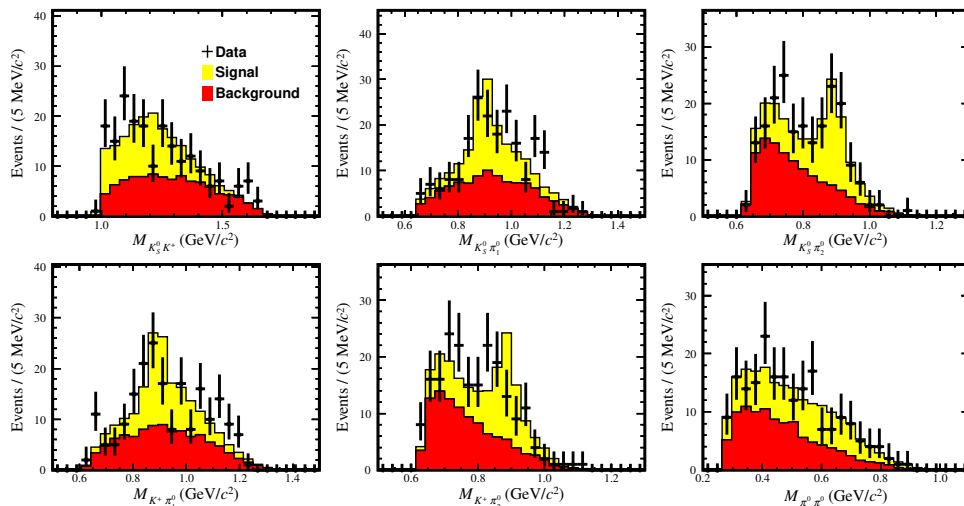


Fig. 5. Comparisons of  $M_{KK}$ ,  $M_{K\pi}$ , and  $M_{\pi\pi}$  for  $D_s^+ \rightarrow K_S^0 K^+ \pi^0 \pi^0$ . The points with error bars are data, the yellow filled histograms are signal, and the red filled histograms are simulated backgrounds from the inclusive MC sample. Events have been further required to satisfy  $1.943 < M_{\text{sig}} < 1.983 \text{ GeV}/c^2$ .

the quoted branching fractions of  $D_s^{*-} \rightarrow \gamma(\pi^0)D_s^+$  be  $\pm 1\sigma$  affects the DT efficiencies by 0.2%, which is assigned as a systematic uncertainty.

The uncertainties due to limited MC statistics are 0.7% and 0.9% for  $D_s^+ \rightarrow K_S^0 K_S^0 \pi^+ \pi^0$  and  $D_s^+ \rightarrow K_S^0 K^+ \pi^0 \pi^0$ , respectively. Due to different reconstruction environments in the inclusive and signal MC samples, the ST efficiencies determined by the inclusive MC sample may be different from those by the signal MC sample. This may lead to incomplete cancellation of the systematic uncertainties associated with the ST selection, referred to as “tag bias”. Inclusive and signal MC efficiencies are

compared and the tracking and PID efficiencies for kaons and pions are studied for different track multiplicities. The resulting ST-average offsets are assigned as the systematic uncertainties from tag bias and listed in Table 4.

For each signal decay, the total systematic uncertainty is obtained by adding these uncertainties in quadrature. They are assigned to be 11.1% and 9.2% for  $D_s^+ \rightarrow K_S^0 K_S^0 \pi^+ \pi^0$  and  $D_s^+ \rightarrow K_S^0 K^+ \pi^0 \pi^0$ , respectively.

Table 2. Requirements of  $M_{\text{tag}}$ , the fitted yields of ST  $D_s^-$  mesons from data ( $N_{\text{ST}}$ ), the efficiencies of detecting ST  $D_s^-$  mesons and DT events ( $\epsilon_{\text{ST}}$ ,  $\epsilon_{\text{DT}}$  and  $\epsilon_{\text{sig}} \equiv \epsilon_{\text{DT}}/\epsilon_{\text{ST}}$ ) for various tag modes, where the uncertainties are statistical only, and all efficiencies are in unit of % and do not include the branching fractions of the decays of each daughter particle.

Tag mode	$M_{\text{tag}}$ (GeV/ $c^2$ )	$N_{\text{ST}}$ ( $\times 10^3$ )	$\epsilon_{\text{ST}}$	$\epsilon_{\text{DT}, K_S^0 K_S^0 \pi^+ \pi^0}$	$\epsilon_{\text{sig}, K_S^0 K_S^0 \pi^+ \pi^0}$	$\epsilon_{\text{DT}, K_S^0 K^+ \pi^0 \pi^0}$	$\epsilon_{\text{sig}, K_S^0 K^+ \pi^0 \pi^0}$
$K^+ K^- \pi^-$	(1.950, 1.986)	280.5 $\pm$ 0.9	40.87 $\pm$ 0.04	3.20 $\pm$ 0.08	7.84 $\pm$ 0.17	3.10 $\pm$ 0.08	7.59 $\pm$ 0.15
$K^+ K^- \pi^- \pi^0$	(1.947, 1.982)	87.5 $\pm$ 0.9	11.83 $\pm$ 0.02	0.90 $\pm$ 0.04	7.60 $\pm$ 0.34	0.71 $\pm$ 0.04	6.01 $\pm$ 0.25
$\pi^- \pi^+ \pi^-$	(1.952, 1.984)	72.7 $\pm$ 1.3	51.86 $\pm$ 0.09	3.85 $\pm$ 0.09	7.42 $\pm$ 0.15	3.70 $\pm$ 0.09	7.13 $\pm$ 0.14
$K_S^0 K^-$	(1.948, 1.991)	63.6 $\pm$ 0.5	47.37 $\pm$ 0.09	3.49 $\pm$ 0.08	7.36 $\pm$ 0.17	3.30 $\pm$ 0.08	6.97 $\pm$ 0.15
$K_S^0 K^- \pi^0$	(1.946, 1.987)	22.2 $\pm$ 0.6	17.00 $\pm$ 0.07	1.13 $\pm$ 0.05	6.67 $\pm$ 0.24	1.09 $\pm$ 0.05	6.40 $\pm$ 0.24
$K^- \pi^+ \pi^-$	(1.953, 1.983)	34.1 $\pm$ 0.8	45.41 $\pm$ 0.12	3.32 $\pm$ 0.08	7.31 $\pm$ 0.15	3.38 $\pm$ 0.08	7.44 $\pm$ 0.15
$K_S^0 K_S^0 \pi^-$	(1.951, 1.986)	10.9 $\pm$ 0.2	22.51 $\pm$ 0.12	1.21 $\pm$ 0.05	5.37 $\pm$ 0.18	1.26 $\pm$ 0.05	5.60 $\pm$ 0.18
$K_S^0 K^+ \pi^- \pi^-$	(1.953, 1.983)	29.6 $\pm$ 0.4	20.98 $\pm$ 0.07	1.13 $\pm$ 0.05	5.38 $\pm$ 0.19	1.16 $\pm$ 0.05	5.55 $\pm$ 0.19
$K_S^0 K^- \pi^+ \pi^-$	(1.958, 1.980)	15.3 $\pm$ 0.4	18.23 $\pm$ 0.09	0.83 $\pm$ 0.04	4.54 $\pm$ 0.22	1.09 $\pm$ 0.05	6.00 $\pm$ 0.22
$\eta_{\gamma} \gamma \pi^-$	(1.930, 2.000)	39.2 $\pm$ 1.3	48.31 $\pm$ 0.11	3.42 $\pm$ 0.08	7.09 $\pm$ 0.17	3.07 $\pm$ 0.08	6.36 $\pm$ 0.15
$\eta_{\pi^+ \pi^- \pi^0 \pi^-}$	(1.941, 1.990)	11.7 $\pm$ 0.3	23.31 $\pm$ 0.12	1.61 $\pm$ 0.06	6.92 $\pm$ 0.22	1.48 $\pm$ 0.05	6.36 $\pm$ 0.22
$\eta'_{\eta \pi^+ \pi^- \pi^-}$	(1.940, 1.996)	20.0 $\pm$ 0.2	25.17 $\pm$ 0.09	1.63 $\pm$ 0.06	6.48 $\pm$ 0.20	1.50 $\pm$ 0.05	5.96 $\pm$ 0.20
$\eta'_{\gamma} \rho \pi^-$	(1.938, 1.992)	49.9 $\pm$ 1.0	32.45 $\pm$ 0.08	2.41 $\pm$ 0.07	7.43 $\pm$ 0.19	2.15 $\pm$ 0.07	6.61 $\pm$ 0.15
$\eta_{\gamma} \rho \pi^-$	(1.920, 2.006)	77.4 $\pm$ 1.5	19.92 $\pm$ 0.04	1.42 $\pm$ 0.05	7.12 $\pm$ 0.25	1.19 $\pm$ 0.05	5.97 $\pm$ 0.20
$\eta_{\pi^+ \pi^- \pi^0 \rho^-}$	(1.927, 1.997)	23.4 $\pm$ 0.5	9.15 $\pm$ 0.04	0.58 $\pm$ 0.03	6.35 $\pm$ 0.33	0.55 $\pm$ 0.03	6.03 $\pm$ 0.33
$\eta_{\gamma} \gamma \pi^+ \pi^- \pi^-$	(1.946, 1.990)	42.7 $\pm$ 0.3	25.00 $\pm$ 0.07	1.46 $\pm$ 0.05	5.84 $\pm$ 0.20	1.59 $\pm$ 0.06	6.38 $\pm$ 0.20

Table 3. The DT yields in data ( $N_{\text{DT}}$ ), the signal efficiencies ( $\epsilon_{\gamma(\pi^0)\text{sig}}$ ), and the obtained branching fractions ( $\mathcal{B}_{\text{sig}}$ ), where the uncertainties are statistical only.

Signal decay	$D_s^+ \rightarrow K_S^0 K_S^0 \pi^+ \pi^0$	$D_s^+ \rightarrow K_S^0 K^+ \pi^0 \pi^0$
$N_{\text{DT}}$	123.7 $\pm$ 14.1	135.2 $\pm$ 26.2
$\epsilon_{\gamma(\pi^0)\text{sig}}$ (%)	7.22 $\pm$ 0.01	6.79 $\pm$ 0.01
$\mathcal{B}_{\text{sig}}$ ( $\times 10^{-3}$ )	4.08 $\pm$ 0.46	3.32 $\pm$ 0.64

## VII. SUMMARY

By analyzing  $e^+e^-$  collision data corresponding to an integrated luminosity of 7.33 fb $^{-1}$ , collected at  $E_{\text{cm}}$  ranging from 4.128 to 4.226 GeV with the BESIII detector, the hadronic decays  $D_s^+ \rightarrow K_S^0 K_S^0 \pi^+ \pi^0$  and  $D_s^+ \rightarrow K_S^0 K^+ \pi^0 \pi^0$  are observed for the first time. The branching fraction of these two decays are determined as  $\mathcal{B}(D_s^+ \rightarrow K_S^0 K_S^0 \pi^+ \pi^0) = (4.08 \pm 0.46 \pm 0.45) \times 10^{-3}$  and  $\mathcal{B}(D_s^+ \rightarrow K_S^0 K^+ \pi^0 \pi^0) = (3.32 \pm 0.64 \pm 0.31) \times 10^{-3}$ , where the first uncertainties are statistical and the second are systematic. The measured branching fraction of  $D_s^+ \rightarrow K_S^0 K_S^0 \pi^+ \pi^0$  is consistent with that of  $D_s^+ \rightarrow K_S^0 K^+ \pi^0 \pi^0$  within uncertainties. We notice that the  $D_s^+ \rightarrow \bar{K}^{*0} K^{*+}$  decay can proceed to decay into the final states of both  $K_S^0 K_S^0 \pi^+ \pi^0$  and  $K_S^0 K^+ \pi^0 \pi^0$ . However, the  $D_s^+ \rightarrow f_0(980)(\rightarrow K_S^0 K_S^0) \rho^+(\rightarrow \pi^+ \pi^0)$  only decays into  $K_S^0 K_S^0 \pi^+ \pi^0$ , but not  $K_S^0 K^+ \pi^0 \pi^0$ . The difference of the two branching fractions may therefore be caused by the contribution from the  $D_s^+ \rightarrow f_0(980) \rho^+$  decay.

Future amplitude analyses of these decays will provide valuable insights into two-body decay modes involving scalar, vector, axial-vector, and tensor mesons, thereby improving our understanding of quark-level SU(3)-flavor symmetry.

### Acknowledgement

The BESIII Collaboration thanks the staff of BEPCII (https://cstr.cn/31109.02.BEPC) and the IHEP computing center for their strong support. The authors thank Prof. Yu-Kuo Hsiao for helpful discussions. This work is supported in part by National Key R&D Program of China under Contracts Nos. 2023YFA1606000, 2023YFA1606704; National Natural Science Foundation of China (NSFC) under Contracts Nos. 11635010, 11935015, 11935016, 11935018, 12025502, 12035009, 12035013, 12061131003, 12192260, 12192261, 12192262, 12192263, 12192264, 12192265, 12221005, 12225509, 12235017, 12361141819; the Chinese Academy of Sciences (CAS) Large-Scale Scientific Facility Program; Joint Large-Scale Scientific Facility Funds of the NSFC and CAS under Contract No. U2032104; the Excellent Youth Foundation of Henan Scientific Committee under Contract No. 242300421044; the Strategic Priority Research Program of Chinese Academy of Sciences under Contract No. XDA0480600; CAS under Contract No. YSBR-101; 100 Talents Program of CAS; The Institute of Nuclear and Particle Physics (INPAC) and Shanghai Key Laboratory for Particle Physics and Cosmology; ERC under Contract No. 758462; German Research Foundation DFG under Contract No. FOR5327; Istituto Nazionale di Fisica Nucleare, Italy; Knut and Alice Wallenberg Foundation under Contracts Nos. 2021.0174, 2021.0299; Ministry of Development of Turkey under Contract No. DPT2006K-120470; National Research Foundation of Korea under Contract No. NRF-2022R1A2C1092335; National Science and Technology fund of Mongolia; Polish National Science Centre under Contract No. 2024/53/B/ST2/00975; STFC (United Kingdom); Swedish Research Council under Contract No. 2019.04595; U. S. Department of Energy under Contract No. DE-FG02-05ER41374

Table 4. Systematic uncertainties (%) in the branching fraction measurements.

Source	$D_s^+ \rightarrow K_S^0 K_S^0 \pi^+ \pi^0$	$D_s^+ \rightarrow K_S^0 K^+ \pi^0 \pi^0$
$N_{ST}^{\text{tot}}$	0.5	0.5
$\pi^+$ tracking	1.0	...
$\pi^+$ PID	1.0	...
$K^+$ tracking	...	1.0
$K^+$ PID	...	1.0
$\gamma$ and $\pi^0$ reconstruction	3.0	5.0
Best transition $\gamma/\pi^0$ selection	0.4	0.4
$K_S^0$ reconstruction	3.0	1.5
Signal shape	0.4	5.4
Background shape	8.8	1.3
MC generator	4.9	4.9
Quoted branching fractions	0.2	0.2
MC statistics	0.7	0.9
Tag bias	0.3	0.2
Total	11.1	9.2

- [1] P. U. E. Onyisi *et al.* (CLEO Collaboration), *Phys. Rev. D* **88**, 032009 (2013).
- [2] M. Ablikim *et al.* (BESIII Collaboration), *JHEP* **06**, 181 (2021).
- [3] Y. K. Hsiao and C. Q. Geng, *Phys. Lett. B* **770**, 348 (2017).
- [4] Z. Rui, Y. Li and H. n. Li, *JHEP* **05**, 082 (2021).
- [5] Y. K. Hsiao, *Phys. Lett. B* **845**, 138158 (2023).
- [6] M. Ablikim *et al.* (BESIII Collaboration), *Phys. Rev. D* **104**, 032011 (2021).
- [7] M. Ablikim *et al.* (BESIII Collaboration), *Phys. Rev. D* **103**, 092006 (2021).
- [8] S. Navas *et al.* (Particle Data Group), *Phys. Rev. D* **110**, 030001 (2024).
- [9] M. Ablikim *et al.* (BESIII Collaboration), *Nucl. Instrum. Meth. A* **614**, 345 (2010).
- [10] C. H. Yu *et al.*, *Proceedings of IPAC2016, Busan, Korea, 2016*.
- [11] X. Li *et al.*, *Radiat. Detect. Technol. Methods* **1**, 13 (2017); Y. X. Guo *et al.*, *Radiat. Detect. Technol. Methods* **1**, 15 (2017); P. Cao *et al.*, *Nucl. Instrum. Meth. A* **953**, 163053 (2020).
- [12] M. Ablikim *et al.* (BESIII Collaboration), *Chin. Phys. C* **39**, 093001 (2015); *Chin. Phys. C* **46**, 113002 (2022). These articles described the integrated luminosity measurement for data taken at  $\sqrt{s} = 4.189, 4.199, 4.209, 4.219$ , and  $4.226$  GeV. The integrated luminosity values for the other data samples have been obtained by a similar procedure.
- [13] S. Agostinelli *et al.* (GEANT4 Collaboration), *Nucl. Instrum. Meth. A* **506**, 250 (2003).
- [14] S. Jadach, B. F. L. Ward and Z. Was, *Phys. Rev. D* **63**, 113009 (2001); *Comput. Phys. Commun.* **130**, 260 (2000).
- [15] D. J. Lange, *Nucl. Instrum. Meth. A* **462**, 152 (2001); R. G. Ping, *Chin. Phys. C* **32**, 599 (2008).
- [16] J. C. Chen, G. S. Huang, X. R. Qi, D. H. Zhang and Y. S. Zhu, *Phys. Rev. D* **62**, 034003 (2000); R. L. Yang, R. G. Ping and H. Chen, *Chin. Phys. Lett.* **31**, 061301 (2014).
- [17] E. Barberio, B. van Eijk and Z. Was, *Comput. Phys. Commun.* **66**, 115 (1991).
- [18] R. M. Baltrusaitis *et al.* (MARKIII collaboration), *Phys. Rev. Lett.* **56**, 2140 (1986).  
J. Adler *et al.* (MARKIII collaboration), *Phys. Rev. Lett.* **60**, 89 (1988).
- [19] B. C. Ke, J. Koponen, H. B. Li and Y. Zheng, *Ann. Rev. Nucl. Part. Sci.* **73**, 285 (2023)
- [20] M. Ablikim *et al.* (BESIII Collaboration), *Phys. Rev. D* **108**, 112001 (2023)
- [21] M. Ablikim *et al.* (BESIII Collaboration), *Phys. Rev. D* **83**, 112005 (2011).
- [22] M. Ablikim *et al.* (BESIII Collaboration), *Phys. Rev. D* **108**, 092003 (2023)
- [23] M. Ablikim *et al.* (BESIII Collaboration), *Phys. Rev. D* **104**, 032001 (2021).
- [24] M. Ablikim *et al.* (BESIII Collaboration), *Phys. Rev. D* **92**, 112008 (2015).
- [25] M. Ablikim *et al.* (BESIII Collaboration), *Phys. Rev. D* **108**, 092003 (2023).
- [26] M. Ablikim *et al.* (BESIII Collaboration), *Phys. Rev. D* **109**, 032011 (2024).